AGU ADVANCING EARTH AND SPACE SCIENCE

Water Resources Research

RESEARCH ARTICLE
10.1029/2020WR028661

Historical Water Storage Changes Over China's Loess Plateau

Rui Shao[1,2,3], Baoqing Zhang[1], Xiaogang He[4,5], Tongxuan Su[1], Yao Li[1], Biao Long[1], Xuejin Wang[1], Wenjing Yang[1], and Chansheng He[1,6]

[1]Key Laboratory of Western China's Environmental Systems (Ministry of Education), College of Earth and Environmental Sciences, Lanzhou University, Lanzhou, China, [2]Department of Hydraulic Engineering, State Key Laboratory of Hydro Science and Engineering, Tsinghua University, Beijing, China, [3]State Key Laboratory of Simulation and Regulation of Water Cycle in River Basin, China Institute of Water Resources and Hydropower Research, Beijing, China, [4]Water in the West, Woods Institute for the Environment, Stanford University, Stanford, CA, USA, [5]Department of Civil and Environmental Engineering, National University of Singapore, Singapore, Singapore, [6]Department of Geography, Western Michigan University, Kalamazoo, MI, USA

Key Points:

- We use simulated evapotranspiration *(ET)* from the PT-JPL model, observed streamflow and precipitation to quantify ΔS from 1982 to 2009 on 16 catchments over the Loess Plateau, China
- We find that a 44.78% increase in vegetation coverage could reduce ΔS by 37.72%
- Neglecting ΔS on a time scale of about 10 years would have the least impact on the streamflow error simulated by the Budyko framework in the Loess Plateau

Supporting Information:

- Supporting Information S1

Correspondence to:

B. Zhang,
baoqzhang@lzu.edu.cn.

Citation:

Shao, R., Zhang, B., He, X., Su, T., Li, Y., Long, B., et al. (2021). Historical water storage changes over China's Loess Plateau. *Water Resources Research*, *57*, e2020WR028661. https://doi.org/10.1029/2020WR028661

Received 23 AUG 2020
Accepted 4 FEB 2021

Abstract Since 1999, the Loess Plateau, China, has undergone one of the world's largest revegetation programs (Grain for Green Project, GfGP). Revegetation has profound impacts on hydrological cycle and water balance, especially in arid and semi-arid areas. As an essential component of water balance, the long-term change in water storage (ΔS) is generally treated as zero. However, it remains unclear how to define the time scale of "long-term," especially over regions undergoing dramatic vegetation restoration. In this study, we quantify ΔS over the Loess Plateau from 1982 to 2009 from a water balance perspective, with a particular focus on the impact of vegetation on ΔS at different time scales. Results show that a 44.78% increase in vegetation coverage could lead to a 37.72% decrease in ΔS. Moreover, the better the vegetation growth, the lower the ratio of ΔS to precipitation ($\Delta S/P$) in the Loess Plateau. $\Delta S/P$ achieved a local minimum at the 4- to 5-year scale and reached a plateau after 10 years. We further use the Budyko framework to verify the above conclusions. We find that errors of simulated streamflow over 11/16 of catchments become stable after 4–5 years, and all 16 catchments become stable after 10 years. Ignoring ΔS at a 10-year scale has the least influence on water budget closure. These findings highlight the importance of considering time scales when ignoring ΔS in the water balance analysis, especially when the length of measurement is limited.

1. Introduction

Estimating long-term average annual water balance at the catchment scale has been an important scientific problem in hydrology and a reliable method for long-term estimates of evapotranspiration (D. Wang, 2012). Water and vegetation in the catchments have reached equilibrium through long-term evolution, so that there is an inextricable relationship between water balance and vegetation change (Gerten et al., 2004). Changes in vegetation affect the elements of water balance, thus vegetation coverage plays an influential role in regulating regional water balance (Heimann & Reichstein, 2008; Seddon et al., 2016). Precipitation (P), evapotranspiration (ET), streamflow (Q), and water storage changes (ΔS) are important components of water balance estimates. Previous studies (e.g., Shao et al., 2019) have demonstrated that vegetation restoration could lead to increases in regional ET over the Loess Plateau, thus changing the water availability. This could potentially exacerbate tensions between water supply and demand in water-stressed regions. Thus, it can be further hypothesized that the vegetation changes may influence the catchment-scale water balance. In addition, the relationship between ΔS and vegetation may be scale dependent and remains unclear, thus studying the time scale of ΔS in vegetation recovery areas is particularly important.

The Loess Plateau, a typical arid and semi-arid region, accounts for 6.6% of China's total land area and supports 8.5% of the population (Fu et al., 2011). It is one of the most water scarce regions with the most fragile ecosystems in the world (Y. Wang et al., 2011; B. Zhang et al., 2016). In the past, the Loess Plateau, with its sparse vegetation coverage, frequent summer rains and intensive agricultural practices, suffered unprecedented water scarcity, soil erosion and fragile ecosystems (C. Wang et al., 2016; Z. Yang et al., 2016). These ecological and environmental problems significantly affect ecological environment and socio-economic

development (Fu et al., 2011). To improve vegetative conditions, the Chinese government has invested a great deal of human, material, and financial resources in the region for ecosystem restoration. Notably, since 1999, the Loess Plateau, has undergone one of the world's largest revegetation programs (Grain for Green Project, GfGP) to combat soil erosion and enhance vegetation coverage of the Loess Plateau (Feng et al., 2016; X. Han et al., 2010; Qiu et al., 2017; B. Zhang et al., 2012). By 2010, the GfGP has increased vegetation coverage by 25% (Y. Chen et al., 2015; S. Wang et al., 2012). Despite these efforts, in areas with dramatic revegetation in the Loess Plateau, vegetation restoration has also increased regional ET, leading to a reduction in surface water (Feng et al., 2016; Shao et al., 2019). Therefore, it is more urgent to explore the relationship between vegetation restoration and ΔS in order to protect water resources and the long-term ecosystem sustainability in the Loess Plateau.

In many regions of the world, ΔS is an essential element in the variation of water balance on annual or shorter time scales, and could even dominate the distribution of water balance in some extremely arid areas (X. Chen et al., 2013; Eltahir & Yeh, 1999; J. Han et al., 2020; Wu et al, 2017, 2019; Yokoo et al., 2008). For example, Xing et al. (2018) confirmed that ΔS has different effects on water balance over different climatic regions in China. Wu et al. (2019) clarified the impacts of ΔS on ET based on the Budyko framework under varying climatic conditions. Moreover, L. Zhang et al. (2008) elucidated that the carryover of water storage could impact the amount of intraannual streamflow produced, thus affecting the average annual variation in streamflow yield and water balance. Therefore, more attention should be paid to the role of ΔS in water balance. However, due to limited ET and ΔS products, annual evaporation is calculated based on $ET = P - Q$ by assuming steady-state conditions $\Delta S = 0$ (Potter & Zhang, 2009; D. Yang et al., 2009). Moreover, most existing studies have ignored ΔS at different time scales when applying water balance models. For instance, Ning et al. (2019) ignored ΔS at the annual scale due to the lack of significant interannual variation from 2003 to 2008 in the Yellow River Basin. Liang et al. (2015) ignored ΔS on a multi-year scale from 1961 to 2009. H. Yang et al. (2018) ignored ΔS on a 5-year scale from 1981 to 2005. But is it reasonable to ignore ΔS in water balance such as those above? How much error will it cause? This main objective of this study is to investigate the role of ΔS on the water balance over 16 catchments of the Loess Plateau, and the errors caused by ignoring ΔS in hydrological process simulations across multiple time scales.

The well-known Budyko framework is a recommended empirical relationship that has shown significant consistency with long-term water balance data for many catchments around the world (Budyko, 1948, 1974). The Budyko (1974) framework uses a functional equilibrium between atmospheric water demand and supply to express the steady-state hydrological partitioning, with a land surface parameter n that characterizes the relationship between hydrology and climate (Choudhury, 1999; Gerrits et al., 2009). Some functional forms for calculating the relationship between the evaporation ratio (ET/P) and the aridity index (PET/P) have been presented to quantify long-time scale water balance relationships (Creed et al., 2014; Jones et al., 2012; S. Zhang et al., 2018). The Budyko framework has long been recognized as a method for investigating the interactions between hydroclimate and catchment characteristics in long-time scale steady state conditions (Donohue et al., 2007; D. Li et al., 2013; Wu et al., 2017; Xiong & Guo, 2012; D. Yang et al., 2009). There is a strong physical connection between ΔS and the Budyko framework. First of all, a key assumption of the Budyko framework is that the long-term water balance is stable and therefore ΔS can be reasonably treated as zero (Donohue et al., 2010). However, ΔS plays an important role in the partitioning of interannual precipitation. For instance, T. Wang et al. (2018) found that the Budyko framework is reliable for the simulation of Q in humid catchments, but not in nonhumid catchments, which due to ΔS role in water balance. D. Wang and Alimohammadi (2012) analyzed the influence of ΔS on ET and found that ET could be overestimated when ΔS was ignored. Second, ΔS impacts the performance of the Budyko framework differently under different climatic conditions, because the temporal variability of the hydrological response to climatic forcing involves processes specific to different regions (Zeng & Cai, 2016). Although studies have quantified the influence of ΔS on water balance in the Budyko framework, our understanding of the components of water balance and their impact on the performance of the Budyko framework is still inadequate due to the huge variability of most water balance variables and associated hydrological processes, especially in areas with intense vegetation restoration. Moreover, the Budyko framework has few parameters, and it has better interpretability compared to other complicated hydrological models. Therefore, it is worth exploring how ΔS affects the performance of the Budyko framework.

In this study, we use simulated *ET*, measured streamflow (*Q*) and precipitation (*P*) to estimate ΔS over the Loess Plateau. Previously, we extended the PT-JPL model at the regional scale to simulate *ET* with and without vegetation restoration on the Loess Plateau, and reliable results were obtained (Shao et al., 2019). Here, we use this *ET* product to estimate ΔS in the Loess Plateau. We selected 16 catchments to explore the scale-dependent response of ΔS to vegetation changes in the Loess Plateau, which were further validated by the Budyko framework. The objectives of this study were: (1) to analyze the influence of vegetation on ΔS over the Loess Plateau; (2) to quantify the characteristics of ΔS at different time scales by revisiting the water balance; and (3) to investigate errors in estimated streamflow based on the Budyko framework when neglected ΔS at different time scales.

2. Study Area and Data

2.1. Study Area

The study area is the Loess Plateau and its 16 catchments. The Loess Plateau is located west of Taihang Mountain, east of Wushao Ridge, north of Qinling Mountains, and south of the Great Wall (Fang et al., 2019a; Meng et al., 2019). The average altitude is 1,000–1,500 m, and the total area is about 640,000 km^2 (Figure 1a) (Fang et al., 2019; Guo et al., 2019). The Loess Plateau is located at the edge of the temperate monsoon climate zone, which has a subhumid to semi-arid continental monsoon climate. The influence of topography and latitude on temperature shows a decreasing trend from south to north, and the monsoon instability is more prominent (Liang et al., 2015; Shao et al., 2019; Y. Wang et al., 2011; B. Zhang et al., 2014;). The annually averaged precipitation varies from 377 mm in the north to 867 mm in the south (Figure 1b; S. Li et al., 2016). Vegetation types of the Loess Plateau from southeast to northwest are forests, forest grasslands, grasslands, desert grasslands and grassland deserts (Xie et al., 2016). Leaf area index (LAI) is significantly higher in the southeast Loess Plateau relative to the northwest (Figure 1c).

Figure 2a shows the spatial distribution of LAI trends in the Loess Plateau. Vegetation increased significantly in 72.04% of the Loess Plateau from 1982 to 2009, and was mainly distributed across the central and southern parts of the Plateau. In contrast, only 15.27% of the total area experienced decreases in LAI, which was distributed in the western and northern parts of the Loess Plateau. In this study, 16 main catchments across vegetation restoration and surface gradients were selected (Figure 1a). Details of long-term hydrometeorological variables of these catchments are summarized in Table 1. Figure 2b illustrates the average annual trends in LAI from 1982 to 2009 for 16 catchments of the Loess Plateau. The annual mean LAI of the 16 catchments from 1982 to 2009 was 0.66 $m^2 \cdot m^{-2}$ ranging from 0.34 $m^2 \cdot m^{-2}$ (Wudinghe catchment) to 1.21 $m^2 \cdot m^{-2}$ (Beiluohe catchment). Among the 16 catchments, the annual mean LAI of Wudinghe, Huangfuchuan, Jialuhe and Tuweihe catchments did not change significantly over the period 1982–2009. However, robust increases in LAI are found in Fenhe catchment (0.0149 $m^2 \cdot m^{-2}\ yr^{-1}$, $p < 0.01$), Qingjianhe catchment (0.0134 $m^2 \cdot m^{-2}\ yr^{-1}$, $p < 0.01$), Gushanchuan catchment (0.0121 $m^2 \cdot m^{-2}\ yr^{-1}$, $p < 0.01$) and Xinshuihe catchment (0.0114 $m^2 \cdot m^{-2}\ yr^{-1}$, $p < 0.01$). These results reflect the fact that a large amount of farmland has been returned to forest and grass in the Loess Plateau, and the effect of vegetation restoration is remarkable.

2.2. Data

China Meteorological Forcing Data set (CMFD) (J. He, Yang, et al., 2020; K. Yang et al., 2010; http://data.tpdc.ac.cn) was used as regional-scale meteorological input to drive PT-JPL model, which was provided by National Tibetan Plateau Data Center. The spatial resolution of CMFD is 0.1° × 0.1° and the time period is from 1979 to 2015. CMFD covers the entire mainland of China, and we extracted the Loess Plateau for calculation and analysis. This data set combines field observations from China Meteorological Administration, satellite precipitation from the Tropical Rainfall Measuring Mission (TRMM), Global Energy and Water Exchanges-Surface Radiation Budget (GEWEX-SRB), and the Princeton Global Forcing (X. He, Pan et al., 2020; Sheffield et al., 2006). The meteorological data used in this study include temperature, radiation, water vapor pressure, specific humidity, precipitation, and barometric pressure from 1982 to 2009.

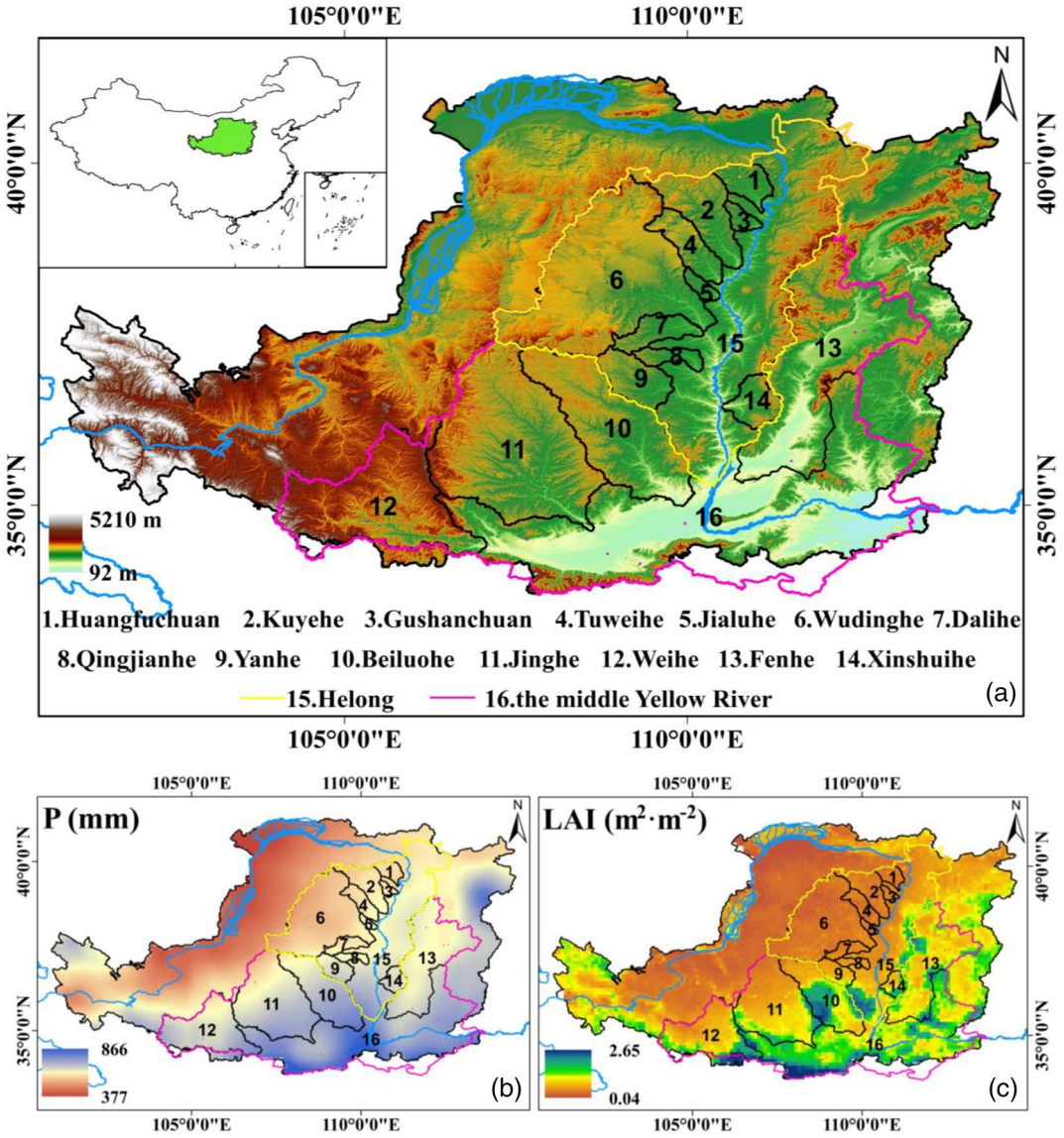

Figure 1. (a) Location of the Loess Plateau and the 16 selected Yellow River catchments. The blue line is the Yellow River and background color shows the elevation. Spatial distribution of (b) annual mean precipitation (*P*) and (c) annual mean leaf area index (LAI) over 1982–2009.

The vegetation data in this study include LAI, enhanced vegetation index (EVI) and normalized difference vegetation index (NDVI). LAI data were obtained from moderate-resolution imaging spectroradiometer (MODIS) LAI product for the period 2001–2015 with a resolution of 500 m (https://lpdaac.usgs.gov/products/mod15a2hv006/) and the advanced very high-resolution radiometer (AVHRR) LAI product for the period 1982–2000 with a resolution of 500 m (http://glcf.umd.edu/data/lai/). NDVI and EVI data were sourced from MODIS with a resolution of 500 m (https://lpdaac.usgs.gov/products/mod13a1v006/).

We used GLEAM *ET* product (https://www.gleam.eu/) to validate the performance of the PT-JPL model on 16 catchments on the Loess Plateau, which is available from the Global Land Evaporation Amsterdam Model. The annual streamflow data from 1982 to 2009 were obtained from the Yellow River Conservancy Commission (http://www.yrcc.gov.cn/). The study period of ΔS was from 1982 to 2009. The reason is that, first of all, the annual streamflow data for 16 catchments on the Loess Plateau are only available before

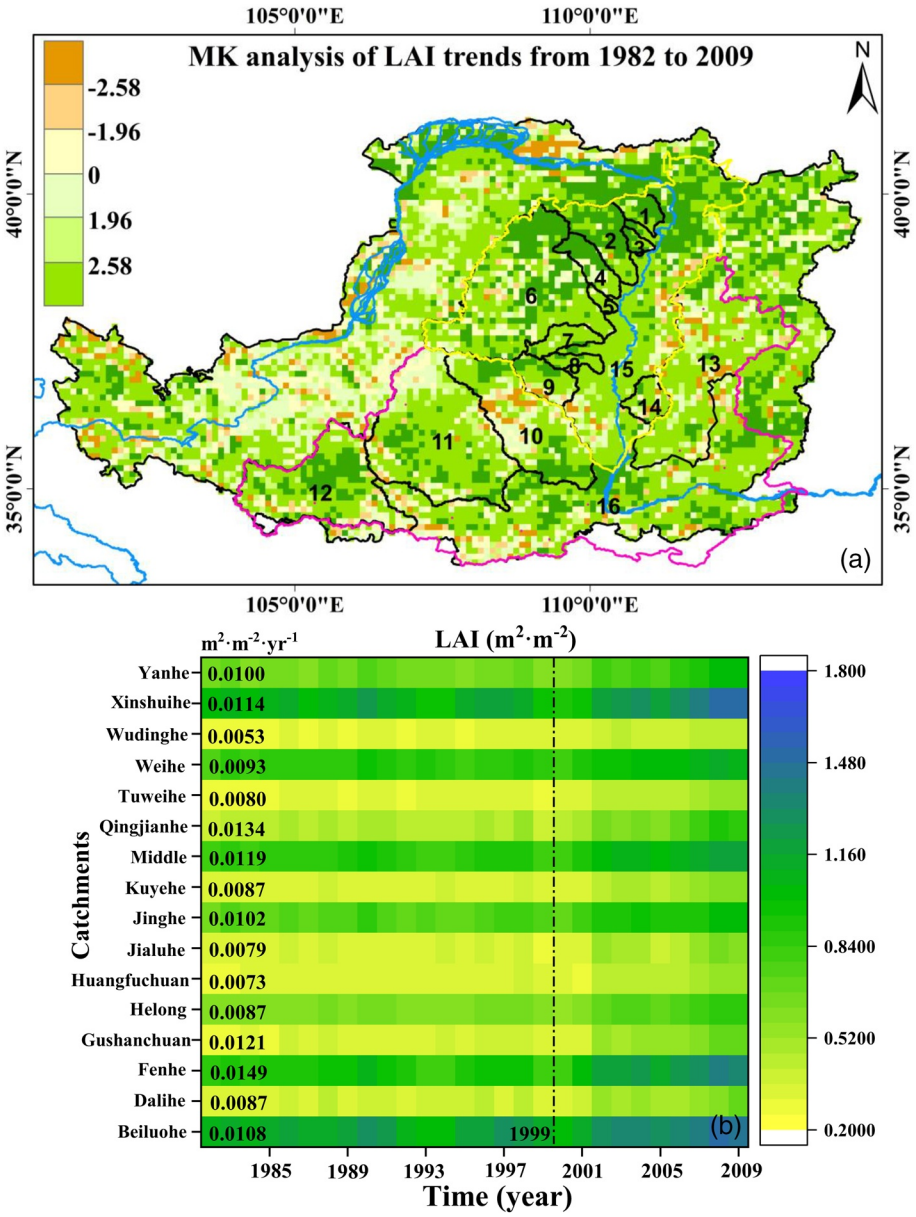

Figure 2. (a) The spatial distribution of Mann-Kendall analysis of annual leaf area index (LAI) trends from 1982 to 2009 on the Loess Plateau; (b) the changes of annual LAI of the 16 catchments from 1982 to 2009 (the vertical dotted line represents 1999). Each grid represents the annual LAI, and the inserted numbers represent the trends of LAI from 1982 to 2009.

2009. Second, *ET* can only be simulated from 1982, due to the lack of LAI and other vegetation index data before 1982.

ERA5-Land monthly mean soil moisture data is created by the European Center for Medium-Range Weather Forecasts (ECMWF). ERA5 is the fifth generation of ECMWF's reanalysis product, which has replaced the ERA-Interim product, and may have greater application potential in the future (Hersbach et al., 2019; C. Wang et al., 2019). ERA5 has been demonstrated to have good performance compared to other reanalysis datasets. Four depths of soil moisture are included in this data: 0–7, 7–28, 28–100, and 100–289 cm. ERA5-Land monthly mean soil moisture data from 0 to 100 cm (0.1° × 0.1°) was used to verify the simulated results in this study (https://cds.climate.copernicus.eu/cdsapp#!/dataset/10.24381/cds.68d2bb30?tab=overview).

Table 1
Long-Term Hydrometeorological Characteristics and Leaf Area Index (LAI) (1982–2009)

ID	Catchment	Gauge station	Area (km^2)	Long-term mean annual value				n
				P (mm)	Q (mm)	PET (mm)	LAI ($m^2 \cdot m^{-2}$)	
1	Huangfuchuan	Huangfu	3,230	399	37	1,141.8	0.37	
2	Kuyehe	Wenjiachuan	8,621	408	60.1	1,162.4	0.39	2.15
3	Gushanchuan	Gaoshiya	1,260	417	50.3	1,194.9	0.41	1.98
4	Tuweihe	Gaojiachuan	3,307	410.5	88.7	1,212.6	0.36	1.31
5	Wudinghe	Dingjiagou	24,682	361.6	34.9	1,257.8	0.34	1.52
6	Jialuhe	Shenjiawan	1,138	436.1	48.4	1,214.8	0.39	1.91
7	Dalihe	Suide	3,861	435	36.6	1,205.4	0.43	1.74
8	Qingjianhe	Yanchuan	3,600	481.5	38.3	1,165.9	0.53	1.98
9	Yanhe	Ganguyi	5,857	511.3	34	1,145.7	0.71	2.22
10	Beiluohe	Zhuangtou	25,723	567.6	35	1,112	1.21	2.55
11	Jinghe	Zhangjiashan	43,106	512.6	33.1	1,090.1	0.81	2.4
12	Weihe	Linjiacun	30,122	508.4	65.4	1,021.5	0.91	2.3
13	Fenhe	Hejin	38,728	476.7	22.6	1,095.7	1.02	3.03
14	Xinshuihe	Daning	4,186	510.8	29.5	1,151.8	1.15	2.45
15	Helong	Longmen and Toudaoguai	136010	445.6	32.9	1,150.3	0.66	2.11
16	Middle Yellow River	Huayuankou and Toudaoguai	366948	518.2	43.9	1,112.7	0.94	2.27

Note: P is obtained from China Meteorological Forcing Data set (CMFD); Q is based on gauge station measurements.
Abbreviations: P, Precipitation; Q, streamflow; PET, potential evapotranspiration; LAI, leaf area index; n, the Budyko land surface parameter.

3. Methods

3.1. The PT-JPL Model

The PT-JPL (Priestley-Taylor Jet Propulsion Laboratory) model is a model developed by Fisher et al. (2008) to estimate actual ET, which reduces potential evapotranspiration (PET) to ET using a large number of indicators based on ecophysiological and atmospheric constraints. The PT-JPL model has a wide range of applications in estimating evaporation (Fisher et al., 2008; Shao et al., 2019).

The net radiation at the regional scale is estimated first, since it is the input data for the PT-JPL model:

$$R_n = R_{n\text{short}} - R_{n\text{long}} \tag{1}$$

$$R_{n\text{short}} = (1 - b) I_t \tag{2}$$

$$R_{n\text{long}} = R_{ld} - R_{lu} \tag{3}$$

$$R_{lu} = \sigma T^4 \tag{4}$$

where R_n, $R_{n\text{short}}$ and $R_{n\text{long}}$ are the surface net radiation, incoming net shortwave radiation and outgoing net longwave radiation ($W \cdot m^{-2}$), respectively; b is surface albedo; I_t is the total incoming shortwave solar radiation ($W \cdot m^{-2}$); R_{lu} and R_{ld} represent the upward and downward longwave radiation ($W \cdot m^{-2}$), respectively; σ is the Stefan-Boltzmann constant (5.67×10^{-8} $W/(m^2 \cdot K^4)$); and T is the air temperature (K) (Allen et al., 1998).

Further estimates of net surface soil radiation and net canopy radiation can be obtained based on the following equations:

$$R_{n\text{soil}} = \left(R_n \exp\left(-k_{R_n} \text{LAI}\right)\right) \tag{5}$$

$$R_{nc} = R_n - R_{n\text{soil}} \tag{6}$$

where k_{R_n} is the extinction coefficient (Fisher et al., 2008); $R_{n\text{soil}}$ and R_{nc} represent the net radiation of surface soil and canopy ($\text{W}\cdot\text{m}^{-2}$), respectively.

PT-JPL model is able to calculate total ET, divide it into transpiration (E_t), soil evaporation (E_b) and interception evaporation (E_i):

$$ET = E_t + E_b + E_i \tag{7}$$

$$E_t = \left(1 - f_{\text{wet}}\right) f_g f_t f_m \alpha \frac{\Delta}{\Delta + \gamma} R_{nc} \tag{8}$$

$$E_b = \left(1 - f_{wet} + f_{sm}\right)\left(1 - f_{\text{wet}}\right)\alpha \frac{\Delta}{\Delta + \gamma}\left(R_{ns} - G\right) \tag{9}$$

$$E_i = f_{\text{wet}} \alpha \frac{\Delta}{\Delta + \gamma} R_{nc} \tag{10}$$

where α is the PT coefficient (taking a value of 1.26); γ represents the psychrometric constant ($\text{kPa}\cdot^\circ\text{C}^{-1}$); Δ represents the slope of the saturated vapor pressure curve ($\text{kPa}\cdot^\circ\text{C}^{-1}$); f_{wet}, f_g, f_t, f_m, and f_{sm} are the relative surface wetness (dimensionless), the green canopy fraction (dimensionless), the plant temperature constraint (dimensionless), the plant moisture constraint (dimensionless), and the soil moisture constraint (dimensionless), respectively; and G is the soil heat flux ($\text{W}\cdot\text{m}^{-2}$).

$$f_t = \exp\left(-\left(\frac{T_{\max} - T_{\text{opt}}}{T_{\text{opt}}^{\ 2}}\right)^2\right) \tag{11}$$

$$f_{\text{wet}} = \text{RH}^4 \tag{12}$$

$$f_g = \frac{f_{APAR}}{f_{IPAR}} \tag{13}$$

$$f_m = \frac{f_{APAR}}{f_{APARmax}} \tag{14}$$

$$f_{sm} = \text{RH}^{\text{VPD}/\beta} \tag{15}$$

where $T_{\max}$ and T_{opt} are the maximum air temperature and optimum plant growth temperature (°C), respectively; RH is the relative humidity (%); VPD is vapor pressure deficit (kPa); β is sensitivity for f_{sm} to VPD; f_{IPAR} and f_{APAR} are the fraction of photosynthesis active radiation (PAR) and the fraction of PAR absorbed by the canopy, respectively (Gao & Li, 2000).

$$e_s = 0.6108e^{\frac{17.27*T_{\min} - 273.15}{T_{\min} - 35.85}} \tag{16}$$

$$e_a = \frac{RH}{100} - e_s. \tag{17}$$

$$VPD = e_s - e_a \tag{18}$$

where T_{min} represents the minimum air temperature (K); e_s and e_a are the saturated water vapor pressure (kPa) and the actual water vapor pressure (kPa), respectively (Shuttleworth, 1993).

$$f_{APAR} = m_1 \mathrm{EVI} + b_1 \tag{19}$$

$$f_{IPAR} = m_2 \mathrm{NDVI} + b_2 \tag{20}$$

where $b_1 = -0.048$, $b_2 = -0.05$, $m_2 = 1$ (Fisher et al., 2008), and m_1 is the parameter to be optimized (Shao et al., 2019).

We conducted two sets of simulations to estimate *ET* with and without vegetation restoration. In the first experiment, *ET* is simulated with vegetation restoration, in which all vegetation parameters can change over time. PT-JPL model was used to simulate actual *ET* with dynamic vegetation. For the latter case, *ET* was calculated assuming no revegetation, with constant vegetation index, temperature, surface albedo, and PT-JPL model temperature control factors.

3.2. Water Storage Changes

A water balance model was used to estimate water storage changes (ΔS) assuming no water flux between two adjacent catchments. The water balance model integrates inflows and outflows on catchments and fundamentally reflects water storage changes in a region (Ward, 1967).

$$\Delta S_i = P_i - ET_i - Q_i \tag{21}$$

where ΔS_i, P_i, ET_i, and Q_i are the annual water storage change (mm), precipitation (mm), evapotranspiration (mm), and streamflow (mm) at year i, respectively.

The multi-year accumulative water storage changes can be calculated according to the annual water storage changes:

$$\Delta S = \frac{1}{N}\sum_{i=1}^{N}\Delta S_i \tag{22}$$

where N is the number of years (D. Wang, 2012).

3.3. Budyko Framework

Previous researchers have developed several mathematical equations to characterize the Budyko framework (Fu, 1996; Pike, 1964). The Choudhury equation is used here (Choudhury, 1999).

$$\frac{ET}{P} = \frac{PET / P}{\left(1 + \left(PET / P\right)^n\right)^{1/n}} \tag{23}$$

where n is the Budyko land surface parameter (dimensionless), which is a function of catchment characteristics, including vegetation coverage, soil characteristics, and climate conditions (H. Yang et al., 2008).

Potential evaporation (*PET*) was calculated by the Penman-Monteith (PM) method (Penman, 1948). The expression is as follows:

$$\lambda PET = \frac{\Delta}{\Delta + \gamma}\left(R_n - G\right) + \frac{\gamma}{\Delta + \gamma} 6.431 + 0.536 U_2 \frac{100 - RH}{100} e_s \tag{24}$$

where λ is the latent heat (MJ/kg); U_2 is the wind speed at 2 m above ground ($\mathrm{m \cdot s^{-1}}$).

3.4. Evaluation and Objective Function

We used the Pearson correlation coefficient (R) and root mean square error ($RMSE$) to analyze the results:

$$R = \frac{\Sigma\left(\theta_i^{\text{obs}} - \bar{O}\right)\left(\theta^{\text{sim}} - \bar{M}\right)}{\sqrt{\Sigma\left(\theta_i^{\text{obs}} - \bar{O}\right)^2 \Sigma\left(\theta^{\text{sim}} - \bar{M}\right)^2}} \tag{25}$$

$$\text{RMSE} = \sqrt{\frac{1}{N}\sum_{i=1}^{N}\left[\theta_i^{\text{obs}} - \theta_i^{\text{sim}}\right]^2} \tag{26}$$

where N represents the number of samples, θ^{sim} represents model simulation, and θ^{obs} represents observation. $\bar{O}$ and $\bar{M}$ are the average of the observed and the simulated value, respectively.

In this study, Mann-Kendall (MK) analysis was used to test the trend of variables. The MK analysis is a widely used nonparametric statistical approach, independent of whether the trend of time series is linear or not, especially for hydrometeorological data that are not normal distribution (Goossens & Berger, 1986). Details of the MK analysis can be found in the supporting information.

4. Results

4.1. Validation of *ET*

Figure 3 demonstrates the comparison between the simulated and observed *ET* for the 12 land cover types. Table S1 provides site details with different land cover types in the supporting information. Results show that there is a significant correlation between the simulated *ET* and observed *ET* for the 12 land cover types ($p < 0.02$). The PT-JPL model was able to accurately simulate the monthly *ET* and trends under different regional conditions and land cover types. Model performance was best in simulating shrub ($R = 0.84$; RMSE = 17.48 mm), farmland ($R = 0.87$. RMSE = 17.42 mm) and forest ($R = 0.89$; RMSE = 22.32 mm).

Validation of annual *ET* by PT-JPL model was performed for 16 catchments in the Loess Plateau. GLEAM *ET* was compared with PT-JPL *ET* for these 16 catchments during 1982–2015 (Figure 4). Results show that the simulated *ET* from PT-JPL model in 16 catchments on the Loess Plateau are significantly correlated with GLEAM *ET* ($p < 0.02$). Among them, the annual *ET* simulated by PT-JPL and GLEAM *ET* have the best correlations in Huangfuchuan, Gushanchuan, Kuyehe and Tuweihe catchments, with correlations of 0.77 ($p < 0.01$; RMSE = 30 mm), 0.78 ($p < 0.01$; RMSE = 29 mm), 0.75 ($p < 0.01$; RMSE = 36 mm) and 0.77 ($p < 0.01$; RMSE = 32 mm) respectively. Overall, the PT-JPL model showed satisfactory results at the catchment scale due to its consistency with the GLEAM *ET* in the 16 catchments over the Loess Plateau.

4.2. Impact of Vegetation Restoration on ΔS

Figures 5a–5c show the long-term (1982–2009) trends of *ET*, *Q*, and *P*, respectively, for the 16 catchments of the Loess Plateau. With the dramatic increase in vegetation by the GfGP, *ET* increased dramatically, and *Q* decreased in the catchments. Whereas *P* decreased on six catchments (Beiluohe, Jinghe, the middle Yellow River, Qingjianhe, Weihe, and Yanhe) and increased on the others. In brief, *ET*, *Q,* and *P* show diverse variations, so that the trend of ΔS is not yet detectable.

ΔS was estimated for 16 catchments on the Loess Plateau based on the water balance equation (Equation 21) and the PT-JPL model, and compared the changes of soil moisture data from ERA5 with ΔS. The results are presented in Figure S1, which shows that the ΔS estimated in this study is significantly related to the changes of soil moisture data from ERA5.

Previous study (e.g., Shao et al., 2019) found that vegetation restoration on the Loess Plateau leads to an increase in regional evaporative water consumption at a rate of 4.90 mm·yr^{-1}. The increase of *ET* caused by vegetation restoration has broken the original water balance, and the change of ΔS caused by vegetation restoration

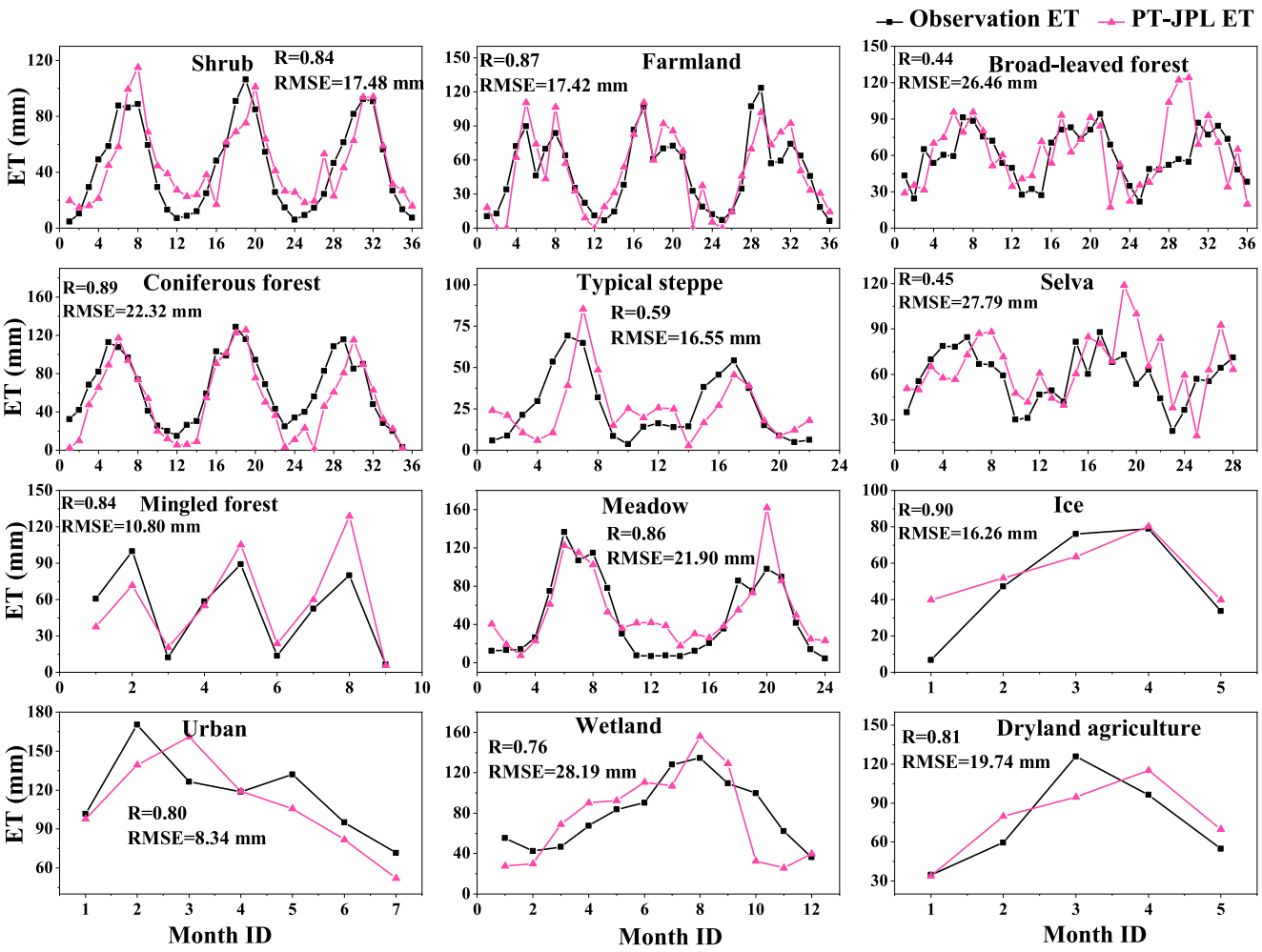

Figure 3. Validation of evapotranspiration *(ET)* for 12 land cover types. The stations corresponding to the different land cover types and their measured times are listed in Table S1. The performance metrics are coefficient of determination (R) and root mean square error (RMSE) on the top of each panel.

in the water balance equation is unknown. Therefore, the effect of vegetation on ΔS was investigated, based on water balance model and two comparative experiments of PT-JPL model. Figure 6 shows that ΔS under revegetation scenario is smaller than that without revegetation in the 16 catchments of the Loess Plateau, which is more robust in the Gushanchuan ($p = 0.01$), Qingjianhe ($p = 0.06$) and Jinghe ($p = 0.07$) catchments at the 90% confidence level. These catchments also correspond to areas with drastic changes in vegetation. However, the difference is not statistically significant in the Weihe ($p = 0.76$), Tuweihe ($p = 0.48$), and Wudinghe ($p = 0.30$) catchments, and vegetation changes in these catchments are also lower than other catchments. Table S2 shows the differences between ΔS with and without revegetation in the 16 catchments of the Loess Plateau (supporting information). On average, a 44.78% increase in vegetation coverage could lead to a 37.72% decrease in ΔS, so the pattern of ΔS should not be ignored in areas where revegetation is strong.

The ratio of ΔS to precipitation ($\Delta S/P$) has been widely used in existing literature (e.g., D. Wang, 2012) as the storage change ratio to indicate the effect of ΔS on water balance in a simplified way. Here, we use $\Delta S/P$ so that our results can be directly compared with previous studies. Second, we conducted robustness checks by comparing $\Delta S/P$ with $\Delta S/PET$, $\Delta S/ET$, and $\Delta S/Q$ in the supporting information (Figure S2). It can be seen that the results of $\Delta S/P$ and $\Delta S/PET$, $\Delta S/ET$, and $\Delta S/Q$ show significant consistency. Therefore, we can reasonably choose $\Delta S/P$ to indicate the effect of ΔS on water balance. The correlation between $\Delta S/P$ and LAI in the catchments was further explored. Figure 7 shows the correlation between the long-term $\Delta S/P$ and annual mean LAI in the 16 catchments of the Loess Plateau from 1982 to 2009. Results showed that there was a statistically significant inverse relationship between $\Delta S/P$ and LAI ($R = -0.83$, $p < 0.001$). In other words, larger LAI is

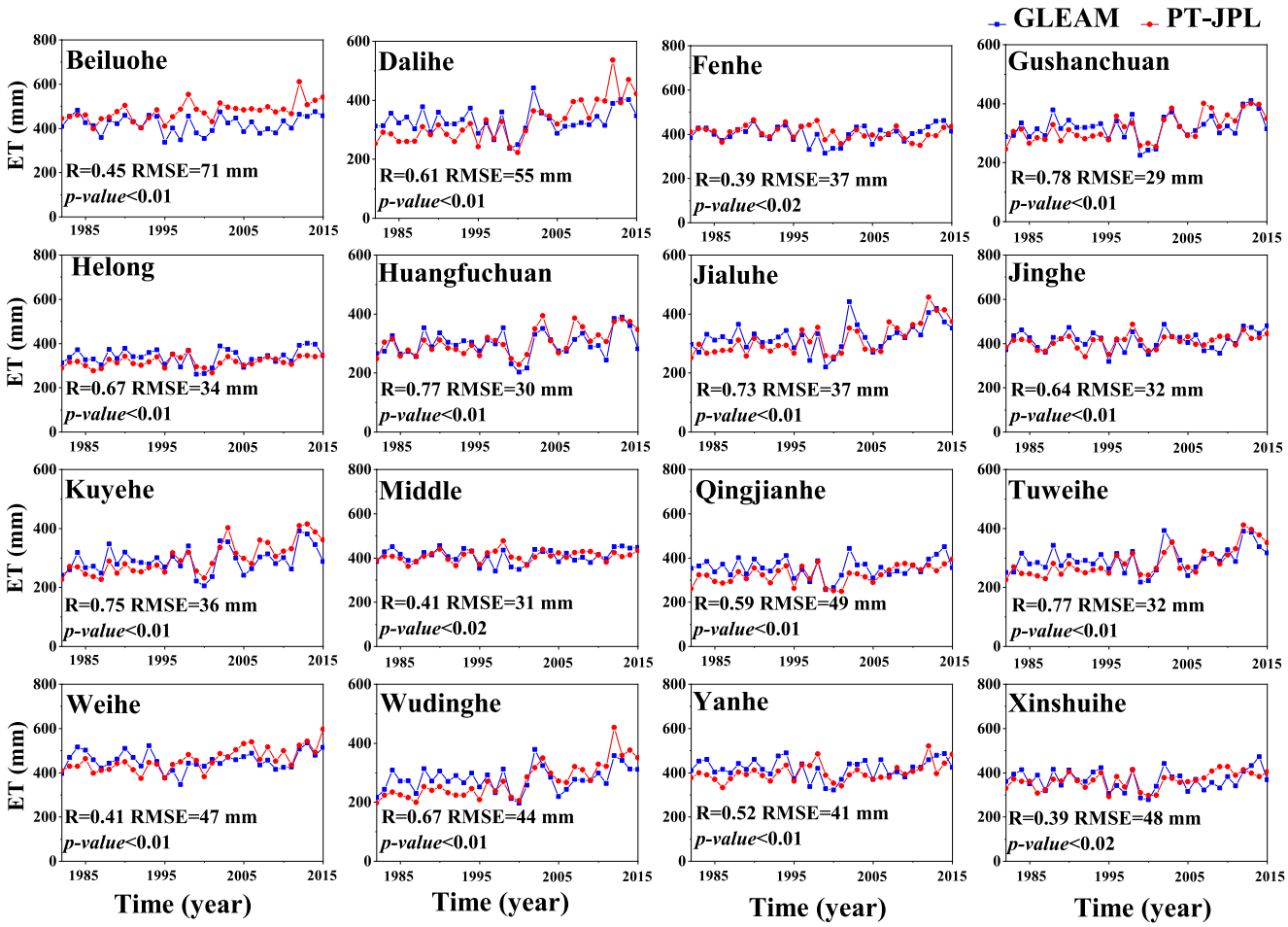

Figure 4. A comparison of the PT-JPL *ET* and GLEAM *ET* for the 16 catchments during 1982–2015. The blue lines are GLEAM *ET*, and the red lines are PT-JPL *ET*.

associated with smaller $\Delta S/P$, which indicates that the smaller the proportion of ΔS in the precipitation is, the smaller the influence on the water balance will be. For example, the annual mean LAI of the Fenhe catchment is large (1.02 $m^2 \cdot m^{-2}$), but its $\Delta S/P$ is small (0.09), and the error caused by ignoring ΔS in water balance may be smaller. On the contrary, the annual mean LAI of the Jialuhe catchment is small (0.39 $m^2 \cdot m^{-2}$), but $\Delta S/P$ is large (0.27). Therefore, the better the vegetation grows, the smaller the effect of ΔS on the water balance.

4.3. Dependence of ΔS on the Time Scale

In this study, in order to investigate the effect of ΔS on the water balance at different time scales, $\Delta S/P$ at different time scales was calculated in the 16 catchments over the Loess Plateau. Figure 8 shows the $\Delta S/P$ in the 16 catchments of the Loess Plateau on time scales of 1–15 years. The $\Delta S/P$ decreases with increasing time scale, reaching a minimum value at the 15-year scale. In addition, it can be found that the $\Delta S/P$ at the 4- to 5-year scale of most catchments reaches a local minimum, reaching a short period of stability (shown by the red dot), and then declines, such as the Huangfuchuan, Jinghe, and Xinshuihe catchments. The $\Delta S/P$ of the 16 catchments is basically stable after the time scale of 10–12 years, indicating that the value of $\Delta S/P$ does not change much after the 10–12 year scale. The first stabilization period is 4–5 years, and the second stabilization period is 10–12 years. Therefore, it can be concluded that in the 16 catchments of the Loess Plateau, ΔS is basically stable and obtains the minimum value above the 10-year scale. In the process of calculating water balance, ignoring the effect of ΔS above the 10-year scale is the smallest, and the 5-year scale is the shortest choice if the time scale cannot reach 10 years.

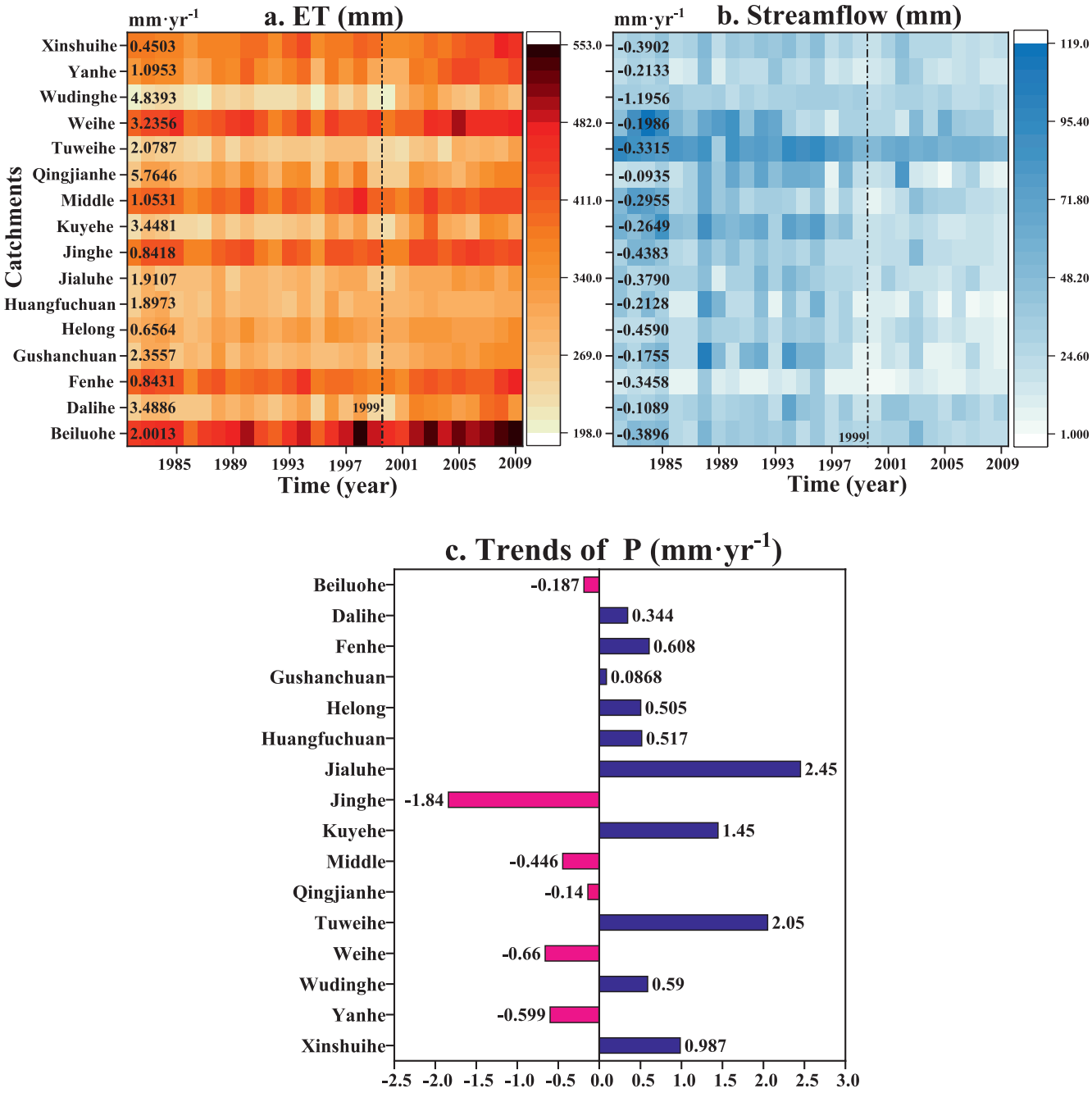

Figure 5. The changes of (a) annual evapotranspiration *(ET)* and (b) annual *Q* of the 16 catchments from 1982 to 2009 (the vertical dotted lines represent 1999). Each grid represents the annual value, and the inserted numbers represent the trends of *ET* and *Q* from 1982 to 2009. (c) The trends of annual precipitation (*P*) of the 16 catchments from 1982 to 2009.

4.4. Influence of ΔS on the Performance of the Budyko Framework

The parameter n was estimated during 1982–2009 based on the long-term average annual *Q*, *P*, and *PET* data (Table 1). Among the 16 catchments, the minimum n value is 1.31 (the Tuweihe catchment), the maximum is 3.03 (the Fenhe catchment) and the average value is 2.00. Geographically, n is higher in the south of the Loess Plateau ($n = 2.55$ for the Beiluohe catchment) and lower in the north ($n = 1.31$ for the Tuweihe catchment). For similar *PET* and *P*, higher n indicates lower *Q* and higher *ET*. As an example, in the Kuyehe and Tuweihe catchments, the Tuweihe catchment has a higher *Q* than the Kuyehe catch-

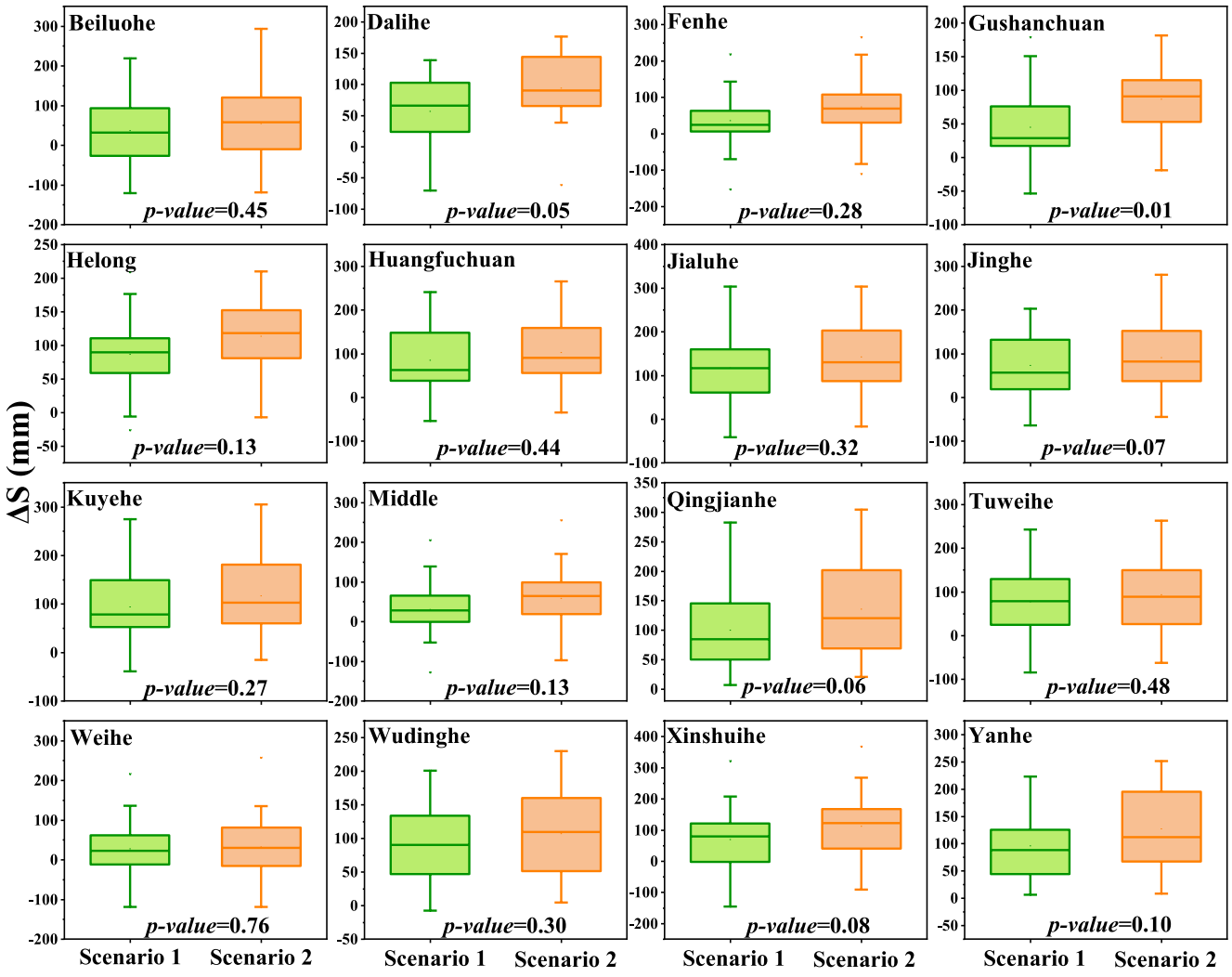

Figure 6. Impacts of vegetation changes on changes in the water storage (ΔS) in the 16 catchments of the Loess Plateau during 1982–2009. Scenarios 1 and 2 indicate experiment of ΔS with and without revegetation, respectively. Box plots show the distributions of annual ΔS from 1982 to 2009.

ment, but the long-term mean annual P and PET for 1982–2009 in the Tuweihe catchment (410.5 and 1,212.6 mm, respectively) are similar to those in the Kuyehe catchment (408.0 and 1,162.4 mm, respectively), which can be explained by a lower n (Table 1). The same example can be given: The Weihe and Fenhe catchments.

Based on the above results, streamflow from the 16 catchments of the Loess Plateau was investigated at different time scales (1–15 years) by the Budyko framework. Simulation results are compared with the measured streamflow (Figure 9). Results demonstrate that the longer the time scale, the lower the RMSE. It further illustrates that the longer the time scale, the less impact of ignoring ΔS on the Budyko framework. In some catchments, there was a turning point in the change of RMSE at the 4- to 5-year scale. For example, the RMSE decreased rapidly on the 1- to 5-year scale in the Huangfuchuan, Xinshuihe and Yanhe catchments but tended to be flat after the 5-year scale. RMSE becomes stable after 10 years over catchments including the Fenhe, Jialuhe, and Tuweihe catchments. In summary, ignoring ΔS at different time scales will have a certain impact on the Budyko framework and cause a certain error, which is catchment dependent. Based on Figures 8 and 9, ignoring ΔS for an analysis period of longer than 10 years has reduced most of the errors, which is consistent with the conclusions drawn by $\Delta S/P$ at different time scales.

In order to explore the correlation between the RMSE of streamflow simulated by the Budyko framework and the $\Delta S/P$ at different time scales, we compared the RMSE of the Budyko framework for the simu-

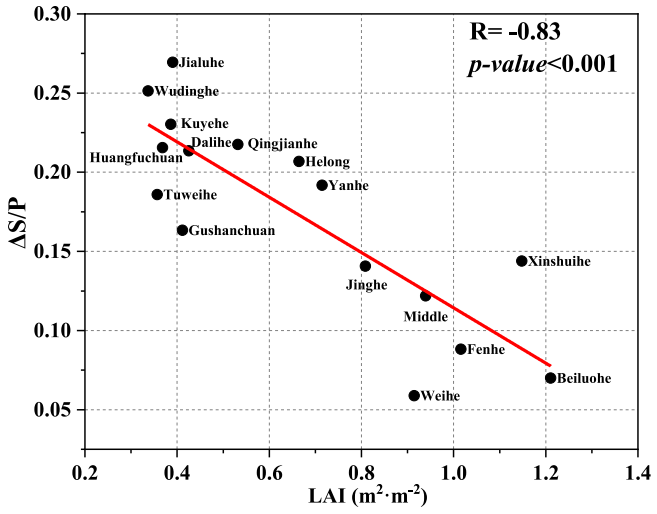

Figure 7. Correlation between long-term (1982–2009) averaged leaf area index (LAI) and $\Delta S/P$ in the 16 catchments over the Loess Plateau. The red line represents the fitting line.

lated streamflow and $\Delta S/P$ in the 16 catchments of the Loess Plateau (Figure 10). The results show that the relationships between RMSE and $\Delta S/P$ are quadratic for the 16 catchments. When $\Delta S/P$ reaches a certain value, RMSE can obtain the minimum value. Then we can find the time scale corresponding to the minimum RMSE. Based on the results in Figure 10, Table 2 shows the time scales corresponding to the minimum RMSE of the Budyko framework simulation results in the 16 catchments of the Loess Plateau. We find that 11 out of 16 catchments including the Beiluohe, Dalihe and Jialuhe catchments achieved the minimum RMSE at a time scale of 9–12 years. Four catchments including the Fenhe, Huangfuchuan, Kuyehe and Gushanchuan catchments achieved the minimum value of RMSE at the time scale longer than 15 years. The minimum time scale that one catchment achieves the minimum RMSE value is found in Yanhe. Although differences exist in the simulation performance of Budyko framework on different time scales, ΔS is ignored in the water balance at a scale of about 10 years, which has the least impact on the analysis of Budyko framework in the Loess Plateau.

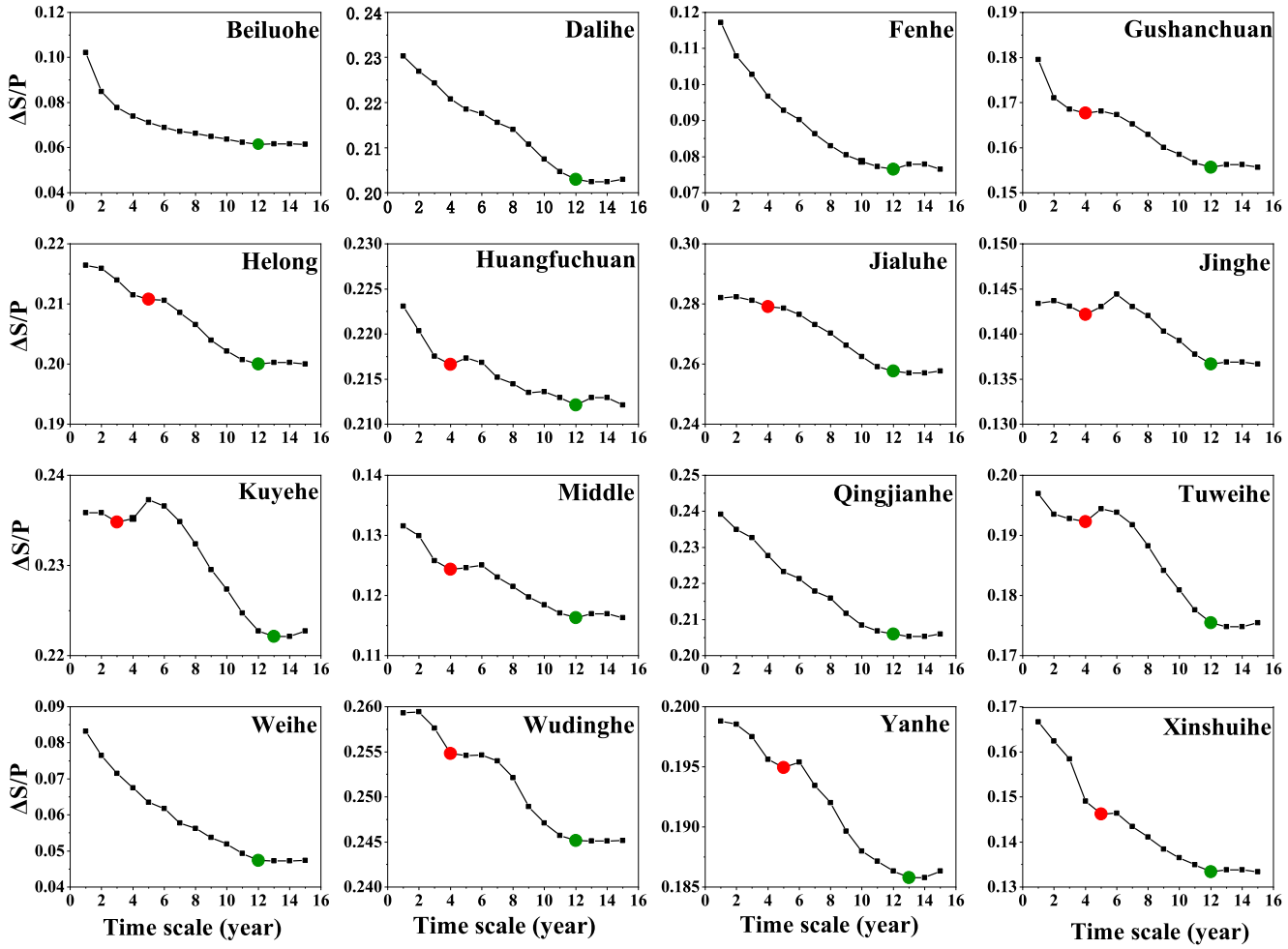

Figure 8. $\Delta S/P$ on different time scales in the 16 catchments of the Loess Plateau. The red dots indicate local minimum on 4- to 5-year scale, and the green dots indicate local minimum after 10-year scale.

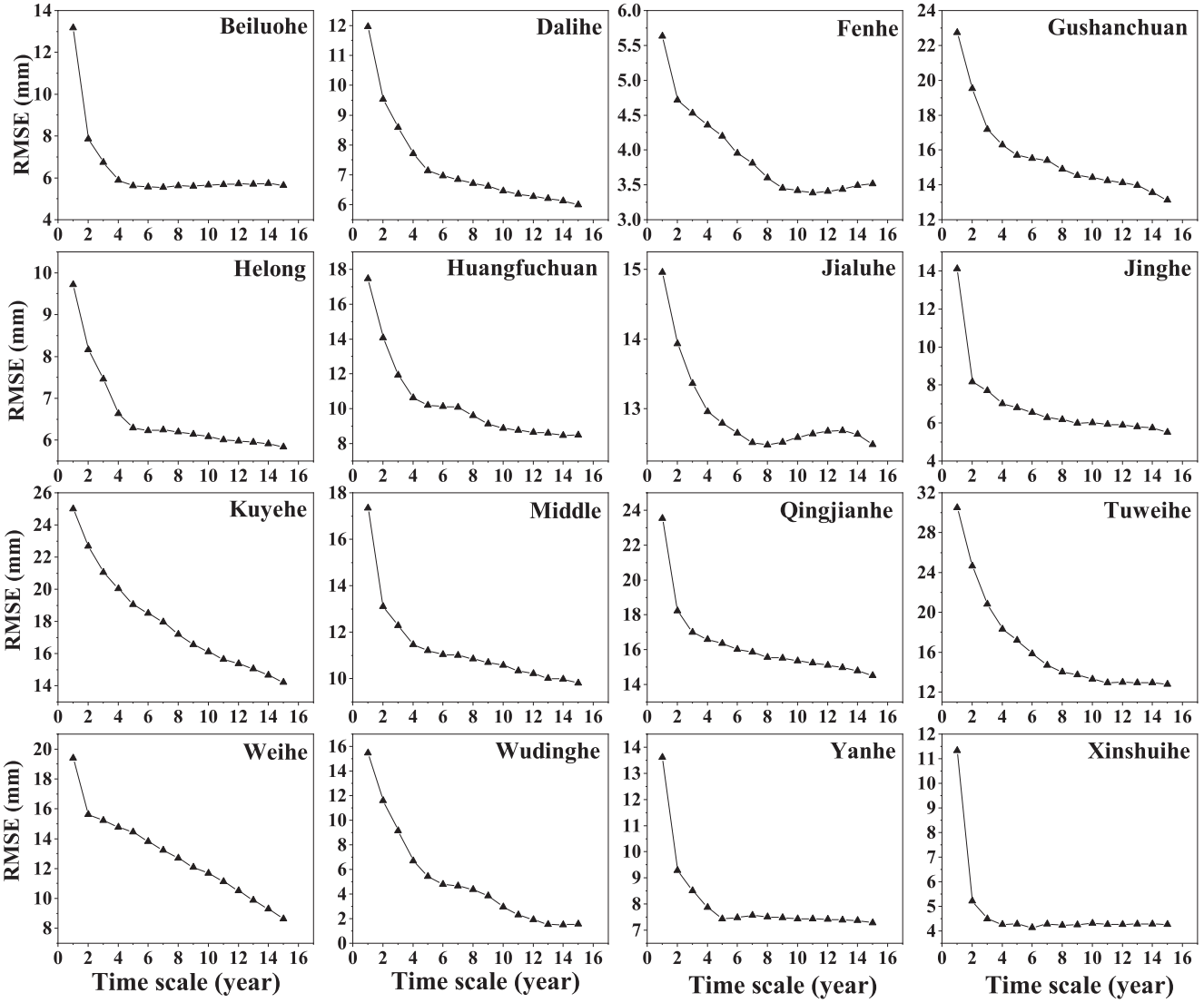

Figure 9. RMSE of the observed streamflow and estimated streamflow by the Budyko framework in the 16 catchments of the Loess Plateau.

5. Discussion

5.1. Effects of Vegetation on ΔS

This study explores the importance of ΔS by incorporating water balance into the Budyko framework. However, the process of vegetation restoration has seldom been studied within the Budyko framework. Our previous study (e.g., Shao et al., 2019) elucidated the importance of vegetation restoration in the inter-annual variability in evaporative water consumption, and confirmed that dramatic changes in vegetation due to the GfGP would lead to an increased evaporative water consumption. Dramatic changes in evapotranspiration on the Loess Plateau have an immediate effect on the water balance in the catchment, which indirectly affect ΔS. Thus, the relationship between ΔS and vegetation should be valued, in order to improve the water balance. Unfortunately, we did not consider the streamflow without vegetation restoration when we studied the effect of revegetation on ΔS. As our objective is to quantify the impact of vegetation restoration on ΔS ($P - ET - Q = \Delta S$), in the water balance equation, only the simulated ET considers the impact of revegetation and we assume that the effect of revegetation on Q can be neglected. The reasons are as follows: first, the change of Q caused by vegetation change is relatively small; second, it is difficult for us to simulate Q without revegetation in a counterfactual world, because the change of vegetation has an indirect effect

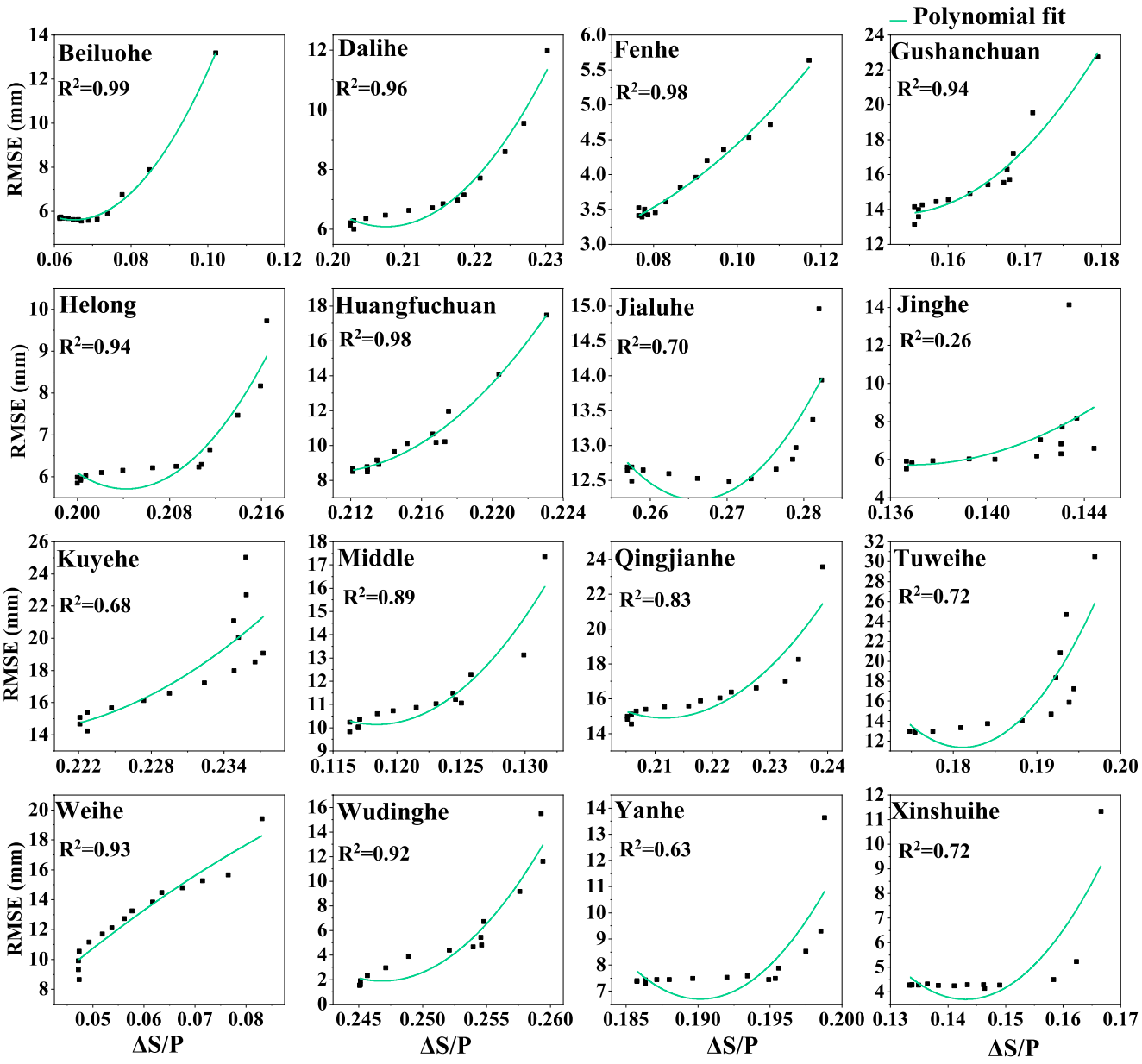

Figure 10. The correlation between the RMSE of streamflow simulated by the Budyko framework and the $\Delta S/P$ at different time scales in the catchments of the Loess Plateau. The green lines represent the polynomial fitting lines.

on the streamflow by affecting *ET*, and other factors can also affect it. For example, the water withdrawal from the Yellow River between the Toudaoguai and Longmen Hydrologic Gauge Stations increased from 1.04×10^9 m^3 to 1.92×10^9 m^3 between 2000 and 2012 to meet the requirements of industrial and agricultural development (YRCC, 2000, 2012). Therefore, it is reasonable to ignore the decrease of streamflow caused by vegetation restoration in the water balance equation.

5.2. Characteristics of ΔS at Different Time Scales

The above results have showed that ΔS was relatively large in most catchments of the Loess Plateau. Possible reasons for this can be explained as the following. First, it is possible that the time scale used in this study is not sufficiently long. Longer-term catchment data may better reflect water balance. In future, ΔS calculated over a longer time scale will be needed. In addition, there could be lateral flows between two

Table 2
Time Scale Values of ΔS/P Corresponding to Minimum RMSE of Budyko Framework Simulated Streamflow in the 16 Catchments of the Loess Plateau

ID	Catchment	$\Delta S/P$	Time scale (year)
1	Huangfuchuan	0.210	15+
2	Kuyehe	0.215	15+
3	Gushanchuan	0.150	15+
4	Tuweihe	0.181	10
5	Wudinghe	0.247	10
6	Jialuhe	0.266	9
7	Dalihe	0.207	10
8	Qingjianhe	0.212	9
9	Yanhe	0.143	7
10	Beiluohe	0.065	9
11	Jinghe	0.137	12
12	Weihe	0.049	11
13	Fenhe	0.042	15+
14	Xinshuihe	0.190	9
15	Helong	0.204	9
16	Middle Yellow River	0.118	10

adjacent catchments that influence ΔS, which are not considered in this study. The water balance equation used in our study is based on the assumption of a closed catchment. If lateral flows exist, this will cause nonclosure of catchment and therefore violate the above key assumption. Currently, it is difficult to obtain any measurement of lateral flows.

5.3. Potential Application of the Results

The Budyko framework assumes ΔS can be ignored based on the long-term averaged water balance, however, water availability is not solely dependent on P at a shorter time scale, as ΔS plays an essential role in balancing the water budget. On the annual scale, the estimates of ET without consideration of ΔS are biased (Istanbulluoglu et al., 2012; T. Wang et al., 2009). Wu et al. (2019) confirmed that the original Budyko framework fails to accurately quantify ET variations in most catchments with significant errors at annual scales due to the effects of ΔS. In order to reduce the errors of ignoring ΔS on the model results, different researchers ignore ΔS on different time scales. For instance, H. Yang et al. (2018) ignored ΔS at a 5-year scale in the application of the Budyko framework, while C. Wang et al. (2019) ignored ΔS at the scale of 29-years of 1981–2009, on the Loess Plateau. It was generally believed that ΔS is smaller compared to the other components of the water balance (i.e., P, Q, and ET) over the multi-year time scale (Roderick & Farquhar, 2011), but it was not clear how many years at least the ideal deviation can be achieved by ignoring ΔS.

Moreover, some researchers used the water balance equation to estimate ET and took it as the true value to verify the simulated ET or Q, still ignoring the effect of ΔS at different time scales. For example, B. Zhang et al. (2020) reported that catchment-scale ET can be quantified based on water balance at the annual time scale, using annual precipitation minus streamflow ($ET = P - Q$; ignoring ΔS). ET estimation methods based on surface water balance have been used extensively in the study of surface hydrology, for example, in validating satellite-retrieved ET (Yang et al., 2012, 2015; B. Zhang et al., 2020). However, ET estimates based on surface water balance is not equal to the observed value measured by the flux towers due to the neglect of ΔS in the water balance model. Our results confirmed that a longer time scale can indeed reduce the effect of ΔS on water balance, but in some cases long time scale does not apply to some analyses (e.g., short research period or to analyze the change of time scale), then we need an intermediate time scale to solve the error due to the ignorance of ΔS.

6. Conclusions

Vegetation changes since the GfGP have a significant impact on the water balance of the Loess Plateau. This study uses the water balance model of the 16 catchments in the Loess Plateau and simulated the ET with and without vegetation based on the PT-JPL model to study how vegetation restoration affects the water storage changes (ΔS). We further verify the results by the Budyko framework. Results show that increased vegetation will reduce ΔS in the catchments, and the better the vegetation growth in the catchments, the lower the $\Delta S/P$, in other words, the smaller the effect of ΔS on the catchment water balance. Considering ΔS at different time scales in the Loess Plateau, $\Delta S/P$ decreases with a longer time scale. It achieved a local minimum on the 4- to 5-year scale and reached a plateau after 10 years. Further verifying the above conclusions based on the Budyko framework, it is found that the RMSE of the simulated streamflow by the Budyko framework and measured streamflow will become stable after 4- to 5-year scale, and some catchments will become stable after 10 years. There is the least influence on the Budyko framework when ignoring ΔS at a 10-year scale in most catchments on the Loess Plateau. Our results confirmed that a longer time scale can indeed reduce the effect of ΔS on water balance, but such long-time scales may not apply to analysis constrained by short periods. In these cases, researchers will need to carefully specify the time scale to minimize the error due to the ignorance of ΔS.

Data Availability Statement

All data in this study were correctly referenced. Thanks to the Yellow River Conservancy Commission in China for providing measured streamflow data (http://www.yrcc.gov.cn/). Thanks to Hydrometeorology Group of the Institute of Tibetan Plateau Research Chinese Academy of Sciences for the China Meteorological Forcing Data set (CMFD) (http://westdc.westgis.ac.cn/data/7a35329c-c53f-4267-aa07-e0037d913a21). The GLEAM *ET* product was provided by the Global Land Evaporation Amsterdam Model (https://www.gleam.eu/). The flux tower-measured data were obtained from the Chinese FLUX Observation and Research Network (http://www.chinaflux.org/index.aspx). The MODIS data set and the AVHRR data set were obtained from the Moderate Resolution Imaging Spectroradiometer (https://modis.gsfc.nasa.gov/) and the NASA Distributed Active Archive Center (DAAC) at NSIDC (https://nsidc.org/data/avhrr), respectively. ERA5-Land monthly mean soil moisture data were obtained from the European Center for Medium-Range Weather Forecasts (https://cds.climate.copernicus.eu/cdsapp#!/dataset/10.24381/cds.68d2bb30?tab=overview).

Acknowledgments
This work was co-supported by the National Natural Science Foundation of China (grant nos. 42041004, 42022001, 41877150, and 42030501), the National Key Research and Development Project of China (grant no. 2020YFA0608403), and the Strategic Priority Research Program of Chinese Academy of Sciences (grant no. XDA20100102).

References

Allen, R. G., Pereira, L. S., Raes, D., & Smith, M. (1998). Crop evapotranspiration: Guidelines for computing crop water requirements. *FAO irrigation and drainage paper No. 56* (pp. 300). Rome, Italy: FAO.

Budyko, M. I. (1948). *Evaporation under natural conditions*. Jerusalem: Isr. Program for Science.

Budyko, M. I. (1974). *Climate and Life*. San Diego, CA: Academic Press.

Chen, X., Alimohammadi, N., & Wang, D. (2013). Modeling interannual variability of seasonal evaporation and storage change based on the extended Budyko framework. *Water Resources Research*, *49*(9), 6067–6078. https://doi.org/10.1002/wrcr.20493

Chen, Y., Wang, K., Lin, Y., Shi, W., Song, Y., & He, X. (2015). Balancing green and grain trade. *Nature Geoscience*, *8*(10), 739–741. https://doi.org/10.1038/ngeo2544

Chen, Y., Yang, K., Tang, W., Qin, J., & Zhao, L. (2012). Parameterizing soil organic carbon's impacts on soil porosity and thermal parameters for Eastern Tibet grasslands. *Science China Earth Sciences*, *55*(06), 1001–1011. https://doi.org/10.1007/s11430-012-4433-0

Choudhury, B. J. (1999). Evaluation of an empirical equation for annual evaporation using field observations and results from a biophysical model. *Journal of Hydrology*, *216*(1–2), 99–110. https://doi.org/10.1016/S0022-1694(98)00293-5

Creed, I. F., Spargo, A. T., Jones, J. A., Buttle, J. M., Adams, M. B., Beall, F. D., & Yao, H. (2014). Changing forest water yields in response to climate warming: results from long-term experimental watershed sites across North America. *Global Change Biology*, *20*(10), 3191–3208. https://doi.org/10.1111/gcb.12615

Donohue, R. J., McVicar, T. R., & Roderick, M. L. (2009). Climate-related trends in Australian vegetation cover as inferred from satellite observations, 1981–2006. *Global Change Biology*, *15*(4), 1025–1039. https://doi.org/10.1111/j.1365-2486.2008.01746.x

Donohue, R. J., McVicar, T. R., & Roderick, M. L. (2010). Assessing the ability of potential evaporation formulations to capture the dynamics in evaporative demand within a changing climate. *Journal of Hydrology*, *386*(1–4), 186–197. https://doi.org/10.1016/j.jhydrol.2010.03.020

Donohue, R. J., Roderick, M. L., & McVicar, T. R. (2007). On the importance of including vegetation dynamics in Budyko's hydrological model. *Hydrology and Earth System Sciences*, *11*(2), 983–995. https://doi.org/10.1016/j.jhydrol.2010.03.020

Eltahir, E. A. B., & Yeh, P. A. J. F. (1999). On the asymmetric response of aquifer water level to floods and droughts in Illinois. *Water Resources Research*, *35*(4), 1199–1217. https://doi.org/10.1029/1998WR900071

Fang, W., Huang, S., Huang, Q., Huang, G., Wang, H., Leng, G., & Guo, Y. (2019a). Probabilistic assessment of remote sensing-based terrestrial vegetation vulnerability to drought stress of the Loess Plateau in China. *Remote Sensing of Environment*, *232*. 111290. https://doi.org/10.1016/j.rse.2019.111290

Feng, X., Fu, B., Piao, S., Wang, S., Ciais, P., Zeng, Z., & Wu, B. (2016). Revegetation in China's Loess Plateau is approaching sustainable water resource limits. *Nature Climate Change*, *6*(11), 1019–1022. https://doi.org/10.1038/nclimate3092

Fisher, J. B., Tu, K. P., & Baldocchi, D. D. (2008). Global estimates of the land-atmosphere water flux based on monthly AVHRR and ISLSCP-II data, validated at 16 FLUXNET sites. *Remote Sensing of Environment*, *112*(3), 901–919. https://doi.org/10.1016/j.rse.2007.06.025

Fu, B. (1996). On the calculation of evaporation from land surface in mountainous areas. *Scientia Meteorologica Sinica*, *6*(4), 328–335.

Fu, B., Liu, Y., Lu, Y. H., He, C., Zeng, Y., & Wu, B. (2011). Assessing the soil erosion control service of ecosystems change in the Loess Plateau of China. *Ecological Complexity*, *8*(4), 284–293. https://doi.org/10.1016/j.ecocom.2011.07.003

Gao, B., & Li, R. (2000). Quantitative improvement in the estimates of NDVI values from remotely sensed data by correcting thin cirrus scattering effects. *Remote Sensing of Environment*, *74*(3), 494–502. https://doi.org/10.1016/S0034-4257(00)00141-3

Gerrits, A. M. J., Savenije, H. H. G., Veling, E. J. M., & Pfister, L. (2009). Analytical derivation of the Budyko curve based on rainfall characteristics and a simple evaporation model. *Water Resources Research*, *45*(4), W04403. https://doi.org/10.1029/2008WR007308

Gerten, D., Schaphoff, S., Haberlandt, U., Lucht, W., & Sitch, S. (2004). Terrestrial vegetation and water balance - hydrological evaluation of a dynamic global vegetation model. *Journal of Hydrology*, *286*(1–4), 249–270. https://doi.org/10.1016/j.jhydrol.2003.09.029

Goossens, C. H., & Berger, A. (1986). Annual and seasonal climatic variations over the northern hemisphere and Europe during the last century. *Annales Geophysicae*, *4*(4), 385–400.

Guo, Y., Huang, S., Huang, Q., Wang, H., Fang, W., Yang, Y., & Wang, L. (2019). Assessing socioeconomic drought based on an improved multivariate standardized reliability and resilience index. *Journal of Hydrology*, *568*, 904–918. https://doi.org/10.1016/j.jhydrol.2018.11.055

Han, J., Yang, Y., Roderick, M. L., McVicar, T. R., Yang, D., Zhang, S., & Beck, H. E. (2020). Assessing the steady-state assumption in water balance calculation across global catchments. *Water Resources Research*, *56*(7), e2020WR027392. https://doi.org/10.1029/2020WR027392

Han, X., Tsunekawa, A., Tsubo, M., & Li, S. (2010). Effects of land-cover type and topography on soil organic carbon storage on Northern Loess Plateau, China. *Acta Agriculturae Scandinavica, Section B - Plant Soil Science*, *60*(4), 326–334. https://doi.org/10.1080/09064710902988672

He, J., Yang, K., Tang, W., Lu, H., Qin, J., Chen, Y. Y., & Li, X. (2020). The first high-resolution meteorological forcing dataset for land process studies over China. *Scientific Data*, *7*, 25. https://doi.org/10.1038/s41597-020-0369-y

He, X., Pan, M., Wei, Z., Wood, E. F., & Sheffield, J. (2020). A global drought and flood catalog from 1950 to 2016. *Bulletin of the American Meteorological Society*, *101*(5), E508–E535. https://doi.org/10.1175/BAMS-D-18-0269.1

Heimann, M., & Reichstein, M. (2008). Terrestrial ecosystem carbon dynamics and climate feedbacks. *Nature*, *451*(7176), 289–292. https://doi.org/10.1038/nature06591

Hersbach, H., Bell, B., Berrisford, P., Horányi, A., Sabater, J. M., Nicolas, J., & Dee, D. (2019). Global reanalysis: goodbye ERA-Interim, hello ERA5. *ECMWF newsletter*, *159*, 17–24.

Istanbulluoglu, E., Wang, T., Wright, O. M., & Lenters, J. D. (2012). Interpretation of hydrologic trends from a water balance perspective: The role of groundwater storage in the Budyko hypothesis. *Water Resources Research*, *48*(3), W00H16. https://doi.org/10.1029/2010WR010100

Jones, J. A., Creed, I. F., Hatcher, K. L., Warren, R. J., Adams, M. B., Benson, M. H., & Williams, M. W. (2012). Ecosystem processes and human influences regulate streamflow response to climate change at long-term ecological research sites. *BioScience*, *62*(4), 390–404. https://doi.org/10.1525/bio.2012.62.4.10

Li, D., Pan, M., Cong, Z., Zhang, L., & Wood, E. (2013). Vegetation control on water and energy balance within the Budyko framework. *Water Resources Research*, *49*(2), 969–976. https://doi.org/10.1002/wrcr.20107

Li, S., Liang, W., Fu, B., Lu, Y., Fu, S., Wang, S., & Su, H. (2016). Vegetation changes in recent large-scale ecological restoration projects and subsequent impact on water resources in China's Loess Plateau. *Science of the Total Environment*, *569*, 1032–1039. https://doi.org/10.1016/j.scitotenv.2016.06.141

Liang, W., Bai, D., Wang, F., Fu, B., Yan, J., Wang, S., & Feng, M. (2015). Quantifying the impacts of climate change and ecological restoration on streamflow changes based on a Budyko hydrological model in China's Loess Plateau. *Water Resources Research*, *51*(8), 6500–6519. https://doi.org/10.1002/2014WR016589

Meng, E., Huang, S., Huang, Q., Fang, W., Wu, L., & Wang, L. (2019). A robust method for non-stationary streamflow prediction based on improved EMD-SVM odel. *Journal of Hydrology*, *568*, 462–478. https://doi.org/10.1016/j.jhydrol.2018.11.015

Ning, T., Zhou, S., Chang, F., Shen, H., Li, Z., & Liu, W. (2019). Interaction of vegetation, climate and topography on evapotranspiration modeling at different time scales within the Budyko framework. *Agricultural and Forest Meteorology*, *275*, 59–68. https://doi.org/10.1016/j.agrformet.2019.05.001

Penman (1948). Natural evaporation from open water, bare soil and grass. *Proceedings of the Royal Society of London*, *193*(1032), 120–145. https://doi.org/10.1098/rspa.1948.0037

Pike, J. G. (1964). The estimation of annual run-off from meteorological data in a tropical climate. *Journal of Hydrology*, *2*(2), 116–123. https://doi.org/10.1016/0022-1694(64)90022-8

Potter, N. J., & Zhang, L. (2009). Interannual variability of catchment water balance in Australia. *Journal of Hydrology*, *369*(1-2), 120–129. https://doi.org/10.1016/j.jhydrol.2009.02.005

Qiu, L., Wu, Y., Wang, L., Lei, X., Liao, W., Hui, Y., & Meng, X. (2017). Spatiotemporal response of the water cycle to land use conversions in a typical hilly–gully basin on the Loess Plateau, China. *Hydrology and Earth System Sciences*, *21*(12), 6485–6499. https://doi.org/10.5194/hess-21-6485-2017

Roderick, M. L., & Farquhar, G. D. (2011). A simple framework for relating variations in runoff to variations in climatic conditions and catchment properties. *Water Resources Research*, *47*(12), W00G07. https://doi.org/10.1029/2010WR009826

Seddon, A. W. R., Macias-Fauria, M., Long, P. R., Benz, D., & Willis, K. J. (2016). Sensitivity of global terrestrial ecosystems to climate variability. *Nature*, *531*(7593), 229–232. https://doi.org/10.1038/nature16986

Shao, R., Zhang, B., Su, T., Long, B., Cheng, L., Xue, Y., & Yang, W. (2019). Estimating the increase in regional evaporative water consumption as a result of vegetation restoration over the Loess Plateau, China. *Journal of Geophysical Research: Atmosphere*. *124*(22), 11783–11802. https://doi.org/10.1029/2019jd031295

Sheffield, J., Goteti, G., & Wood, E. F. (2006). Development of a 50-year high-resolution global dataset of meteorological forcings for land surface modeling. *Journal of Climate*, *19*(13), 3088–3111. https://doi.org/10.1175/JCLI3790.1

Shuttleworth, W. J. (1993). Evaporation. In D. R. Maidment (Ed.), *Handbook of hydrology* (pp. 104–155). New York, NY: McGraw-Hill.

Wang, C., Graham, R. M., Wang, K., Gerland, S., & Granskog, M. A. (2019). Comparison of ERA5 and ERA-Interim near-surface air temperature, snowfall and precipitation over Arctic sea ice: effects on sea ice thermodynamics and evolution. *The Cryosphere*, *13*(6), 1661–1679. https://doi.org/10.5194/tc-13-1661-2019

Wang, C., Wang, S., Fu, B., & Zhang, L. (2016). Advances in hydrological modeling with the Budyko framework: A review. *Progress in Physical Geography-Earth and Environment*, *40*(3), 409–430. https://doi.org/10.1177/0309133315620997

Wang, D. (2012). Evaluating interannual water storage changes at watersheds in Illinois based on long-term soil moisture and groundwater level data. *Water Resources Research*, *48*(3), 31–40. https://doi.org/10.1029/2011WR010759

Wang, D., & Alimohammadi, N. (2012). Responses of annual runoff, evaporation, and storage change to climate variability at the watershed scale. *Water Resources Research*, *48*(5), W05546. https://doi.org/10.1029/2011WR011444

Wang, F., Duan, K., Fu, S., Gou, F., Liang, W., Yan, J., & Zhang, W. (2019). Partitioning climate and human contributions to changes in mean annual streamflow based on the Budyko complementary relationship in the Loess Plateau, China. *Science of the Total Environment*, *665*, 579–590. https://doi.org/10.1016/j.scitotenv.2019.01.386

Wang, S., Fu, B., Gao, G., Yao, X., & Zhou, J. (2012). Soil moisture and evapotranspiration of different land cover types in the Loess Plateau, China. *Hydrology and Earth System Sciences*, *16*(8), 2883–2892. https://doi.org/10.5194/hess-16-2883-2012

Wang, T., Istanbulluoglu, E., Lenters, J., & Scott, D. (2009). On the Role of Groundwater and Soil Texture in the Regional Water Balance: An Investigation of the Nebraska Sand Hills. USA. *Water Resources Research*, *45*(10), W10413. https://doi.org/10.1029/2009WR007733

Wang, T., Sun, F., Lim, W. H., Wang, H., Liu, W., & Liu, C. (2018). The Predictability of annual evapotranspiration and runoff in humid and nonhumid catchments over China: Comparison and quantification. *Journal of Hydrometeorology*, *19*(3), 533–545. https://doi.org/10.1175/JHM-D-17-0165.1

Wang, Y., Shao, M., Zhu, Y., & Liu, Z. (2011). Impacts of land use and plant characteristics on dried soil layers in different climatic regions on the Loess Plateau of China. *Agricultural and Forest Meteorology*, *151*(4), 437–448. https://doi.org/10.1016/j.agrformet.2010.11.016

Ward, R. C. (1967). *Principles of hydrology*. London, New York: McGraw-Hill Pub. Co.

Wu, C., Hu, B., Huang, G., & Zhang, H. (2017). Effects of climate and terrestrial storage on temporal variability of actual evapotranspiration. *Journal of Hydrology*, *549*, 388–403. https://doi.org/10.1016/j.jhydrol.2017.04.012

Wu, C., Yeh, P. J., Wu, H., Hu, B. X., & Huang, G. (2019). Global analysis of the role of terrestrial water storage in the evapotranspiration estimated from the budyko framework at annual to monthly time scales. *Journal of Hydrometeorology*, *20*(10), 2003–2021. https://doi.org/10.1175/JHM-D-19-0065.1

Xie, B., Jia, X., Qin, Z., Shen, J., & Chang, Q. (2016). Vegetation dynamics and climate change on the Loess Plateau, China: 1982-2011. *Regional Environmental Change*, *16*(6), 1583–1594. https://doi.org/10.1007/s10113-015-0881-3

Xing, W., Wang, W., Shao, Q., Yong, B., Liu, C., Feng, X., & Dong, Q. (2018). Estimating monthly evapotranspiration by assimilating remotely sensed water storage data into the extended Budyko framework across different climatic regions. *Journal of Hydrology*, *567*, 684–695. https://doi.org/10.1016/j.jhydrol.2018.10.014

Xiong, L., & Guo, S. (2012). Appraisal of Budyko formula in calculating long-term water balance in humid watersheds of southern China. *Hydrological Processes*, *26*(9), 1370–1378. https://doi.org/10.1002/hyp.8273

Yang, D., Shao, W., Yeh, P. J. F., Yang, H., Kanae, S., & Oki, T. (2009). Impact of vegetation coverage on regional water balance in the nonhumid regions of China. *Water Resources Research*, *45*(7), W00A14. https://doi.org/10.1029/2008WR006948

Yang, H., Piao, S., Huntingford, C., Ciais, P., Li, Y., Wang, T., & Chang, J. (2018). Changing the retention properties of catchments and their influence on runoff under climate change. *Environmental Research Letters*, *13*(9), 094019. https://doi.org/10.1088/1748-9326/aadd32

Yang, H., Yang, D., Lei, Z., & Sun, F. (2008). New analytical derivation of the mean annual water-energy balance equation. *Water Resources Research*, *44*(3), W03410. https://doi.org/10.1029/2007WR006135

Yang, K., He, J., Tang, W., Qin, J., & Cheng, C. (2010). On downward shortwave and longwave radiations over high altitude regions: Observation and modeling in the Tibetan Plateau. *Agricultural and Forest Meteorology*, *150*(1), 0–46. https://doi.org/10.1016/j.agrformet.2009.08.004

Yang, Y., Long, D., Guan, H., Liang, W., Simmons, C., & Batelaan, O. (2015). Comparison of three dual-source remote sensing evapotranspiration models during the MUSOEXE-12 campaign: Revisit of model physics. *Water Resources Research*, *51*(5), 3145–3165. https://doi.org/10.1002/2014WR015619

Yang, Y., Shang, S., & Jiang, L. (2012). Remote sensing temporal and spatial patterns of evapotranspiration and the responses to water management in a large irrigation district of North China. *Agricultural and Forest Meteorology*, *164*, 112–122. https://doi.org/10.1016/j.agrformet.2012.05.011

Yang, Z., Zhang, Q., Yang, Y., Hao, X., & Zhang, H. (2016). Evaluation of evapotranspiration models over semi-arid and semi-humid areas of China. *Hydrological Processes*, *30*(23), 4292–4313. https://doi.org/10.1002/hyp.10824

Yokoo, Y., Sivapalan, M., & Oki, T. (2008). Investigating the roles of climate seasonality and landscape characteristics on mean annual and monthly water balances. *Journal of Hydrology*, *357*(3–4), 255–269. https://doi.org/10.1016/j.jhydrol.2008.05.010

YRCC, Yellow River Conservancy Commision. (2000). *Water resources bulletin of the yellow river*. http://www.yrcc.gov.cn/other/hhgb/2000.htm

YRCC, Yellow River Conservancy Commision. (2012). *Water resources bulletin of the yellow river*. http://www.yrcc.gov.cn/other/hhgb/2012szygb/2012szygb.html

Zeng, R., & Cai, X. (2016). Climatic and terrestrial storage control on evapotranspiration temporal variability: Analysis of river basins around the world. *Geophysical Research Letters*, *43*(1), 185–195. https://doi.org/10.1002/2015GL066470

Zhang, B., He, C., Burnham, M., & Zhang, L. (2016). Evaluating the coupling effects of climate aridity and vegetation restoration on soil erosion over the Loess Plateau in China. *Science of the Total Environment*, *539*, 436–449. https://doi.org/10.1016/j.scitotenv.2015.08.132

Zhang, B., Wu, P., Zhao, X., Gao, X., & Shi, Y. (2014). Assessing the spatial and temporal variation of the rainwater harvesting potential (1971–2010) on the Chinese Loess Plateau using the VIC model. *Hydrological Processes*, *28*(3), 534–544. https://doi.org/10.1002/hyp.9608

Zhang, B., Wu, P., Zhao, X., Wang, Y., & Gao, X. (2012). Changes in vegetation condition in areas with different gradients (1980–2010) on the Loess Plateau, China. *Environmental Earth Sciences*, *68*(8), 2427–2438. https://doi.org/10.1007/s12665-012-1927-1

Zhang, B., Xia, Y., Long, B., Hobbins, M., Zhao, X., Hain, C., & Anderson, M. C. (2020). Evaluation and comparison of multiple evapotranspiration data models over the contiguous United States: Implications for the next phase of NLDAS (NLDAS-Testbed) development. *Agricultural and Forest Meteorology*, *280*, 107810. https://doi.org/10.1016/j.agrformet.2019.107810

Zhang, L., Potter, N., Hickel, K., Zhang, Y., & Shao, Q. (2008). Water balance modeling over variable time scales based on the Budyko framework – Model development and testing. *Journal of Hydrology*, *360*(1–4), 117–131. https://doi.org/10.1016/j.jhydrol.2008.07.021

Zhang, S., Yang, Y., McVicar, T. R., & Yang, D. (2018). An analytical solution for the impact of vegetation changes on hydrological partitioning within the budyko framework. *Water Resources Research*, *54*(1), 519–537. https://doi.org/10.1002/2017WR022028